THE ASTROPHYSICAL JOURNAL, 343:135–141, 1989 August 1

RELATION BETWEEN THE IONIZING CONTINUUM AND THE EMISSION LINES IN FAIRALL 9

LUC BINETTE,[1,2] ALMUDENA PRIETO,[2,3] EWA SZUSZKIEWICZ,[2,4] AND WEI ZHENG[2,5]
Received 1988 October 6; accepted 1989 January 18

ABSTRACT

We have studied the evolution of the emission line ratios of a photoionized cloud described by standard BLR parameters which is exposed to a varying ionizing continuum. The hardness of the ionizing distribution was varied by decoupling the UV increase from that of the X-ray component. After many tests using various ionizing distributions, it became apparent that the energy distribution must change in certain specific ways if Lyα/C IV is to increase monotonically with f(1338 Å) as in *Fairall 9*. A distribution composed of a varying 10 eV bump and a constant luminosity X-ray power law can successfully reproduce the observed Lyα/C IV slope. This would be consistent with reported X-ray data only if the varying absorbing column density model were a valid explanation of its variability. We have also considered the possibility that the UV bump may become cooler with luminosity or that the BLR may cover a wide range in U and n_H. We conclude that the geometry of the BLR is a potentially significant factor.

Subject headings: galaxies: individual (Fairall 9) — galaxies: Seyfert — line: formation — ultraviolet: spectra — X-rays: spectra

I. INTRODUCTION

The strong emission lines generated in active galactic nuclei (AGNs) are generally believed to result from the photoionization of nuclear gas by a very intense ultraviolet-X-ray emission continuum referred to as the ionizing continuum. The natural assumption has been that this ionizing continuum, which is not directly observable, is simply the extension of the optical nonstellar continuum in the far UV. At higher energies, the X-ray continuum emission often associated with the AGN phenomenon is also believed to play an important role in producing line emission. The extensive observations of the Seyfert I galaxy Fairall 9 reported by Clavel, Wamsteker, and Glass (1988, hereafter CWG) provide us with interesting clues about the respective roles of the various ionizing components in producing the observed line spectrum. A strong correlation was reported to exist between the Lyα/C IV and Lyα/Mg II line ratios on the one hand and the intensity of the ultraviolet continuum on the other. Between 1978 and 1984, Fairall 9 underwent a dramatic decrease in its UV continuum intensity, while the X-rays decreased by a much smaller factor. The observed increase in the emission line ratio Lyα/C IV which accompanies the UV continuum decline is, however, the opposite of the decrease which photoionization models of the broad line region (BLR) predict (e.g., Mushotzky and Ferland 1984). In this paper we look at ways in which the ionizing continuum could vary in its spectral distribution so as to produce the observed correlations. We start with the simplest approach, decoupling the X-ray component from that of the varying UV continuum, as suggested by Clavel, Wamsteker, and Glass (1988). We experiment with various energy distributions for the UV continuum as well as different luminosity behavior for the X-ray component. We go on to discuss the possible effect of geometrical stratification of the BLR on our results.

II. NUMERICAL CODE AND INPUT PARAMETERS

To derive line fluxes produced by the various ionizing energy distributions, we have employed a new version of the code MAPPINGS previously applied to the NLR (see Binette and Robinson 1987; Binette, Robinson, and Courvoisier 1988). This recent version makes use of the hydrogen transfer solution developed by Zheng (1989) and incorporates a five-level treatment of the hydrogen atom. Although our treatment of the physical processes is largely indebted to Kwan and Krolik (1981), we have implemented other processes important at very high densities described by Ferland and Rees (1988), such as free-free heating (as well as the resulting opacity to incident radiation); induced and three-body recombination of hydrogen; photoelectric absorption which takes into account the effect of induced recombination. The "on-the-spot" approximation is replaced by computing explicitly the diffuse photon field which not only includes recombination continuum photons but emission lines as well. By expanding the code in this way, we can compute line fluxes for densities appropriate to the BLR and within at least the range of densities of the "standard" model of Kwan and Krolik (1981).

In all the calculations reported below we have employed a cloud density of $n_H = 10^{10.5}$ cm^{-3} (i.e., $p \simeq 6 \times 10^{14}$ K cm^{-3}), which corresponds to the high limit of the standard BLR model (see Krolik and Kallman 1988). The results of Robinson and Pérez (1989) indicate that larger densities are not essential to account for the BLR short time lag response to continuum variations. The abundances of metals are "solar"; the values are quoted in Binette, Robinson, and Courvoisier (1988). Although the initial computations assumed nearly ionization-bounded conditions, it was subsequently a simple matter to derive the spectrum at any chosen value of the geometrical thickness as represented by the clouds' column density N_H, given that the cumulative line spectrum was stored as a function of geometrical depth during the "outward" integration

[1] Canadian Institute for Theoretical Astrophysics, Toronto.
[2] Instituto de Astrofísica de Canarias, Tenerife.
[3] ST-ECF is affiliated with the Astrophysics Division, Space Science Department. European Space Agency. ESO, Garching bei München.
[4] Scuola Internazionale Superiore Di Studi Avanzati, Trieste.
[5] Beijing Astronomical Observatory, Academia Sinica, Beijing.

calculations. For canonical values of N_H, only the Mg II line out of those studied here is significantly affected under matter-bounded conditions.

It is often stated that the line spectrum depends more critically on the ionization parameter U than on the details of the energy distribution (see Krolik and Kallman 1988). Our definition of the ionization parameter is

$$U = \frac{1}{n_H c}\int_{\nu_1}^{\infty}\frac{f_\nu}{h\nu}\,d\nu = \frac{Q_t}{4\pi r^2 n_H c} \quad (1)$$

where $h\nu_1 \equiv 1$ Ry is the energy at the Lyman limit, f_ν is the ionizing radiation flux in ergs cm^{-3} s^{-1} Hz^{-1} impinging on a cloud of density n_H at distance r from the central source, Q_t is the total number of ionizing photons below 10 keV emitted by the central source per second, and c the speed of light. We took n_H to be constant within a cloud; any other assumption, constant gas pressure for example, would be arbitrary, given that the cloud density structure is expected to respond to pressure gradients on a time scale longer or comparable to that of the observed continuum variations in Fairall 9.

III. OVERVIEW OF THE OBSERVATIONS

In their study of the continuum spectral distribution in Fairall 9, CWG clearly show the absence of any secular change in the spectral index of the UV continuum, although the continuum level does vary greatly. The spectral index α_{UV} they derived from *IUE* observations within the line-free windows of 1338 Å and 1826 Å, after correction for reddening [$E(B-V) \sim 0.07$], has a mean value of $\alpha_{UV} = -0.46 \pm 0.11$ ($f_\nu \propto \nu^\alpha$). The continuum light curve of Fairall 9 shows the flux at 1338 Å, f(1338 Å), to undergo a secular decrease by a factor Λf(1338 Å), possibly as high as 33 between 1978 and 1984, followed by a partial recovery from the end of 1984. However, if averages of flux measurements at low and high state are taken or if the flux at 1826 Å is considered instead, Λf(1338 Å) is much lower. We infer from the CWG data that Λf(1338 Å) > 20 and estimate the most likely value to be $\simeq$28.

The overall energy distribution of Fairall 9 is characterized by a large energy excess in the UV usually referred to as the "big blue bump" (Elvis *et al.* 1986). This continuum excess is in fact the combination of a "small bump" which peaks at around 3000 Å (Wamsteker *et al.* 1984) and the underlying "big bump" itself which covers a much broader frequency range. The physical origin of the big bump has often been interpreted as thermal emission from an optically thick source such as an accretion disk (see Abramowicz and Szuszkiewicz 1989 and references therein) or photosphere (Camenzind and Courvoisier 1983). Nothwithstanding its physical origin, the extension of the big bump in the unobservable EUV is probably an important, if not the major, component of the ionizing distribution. However, at some point in the EUV, this component must roll over and connect with the 2–6 keV X-rays which are observed to be weaker than the *extrapolated* UV continuum by an order of magnitude. By comparing *EXOSAT* data with all previous X-ray observations, Morini *et al.* (1986) have shown the 1–10 keV flux to have varied much less than the UV. They found no indication of variation in the index of the power-law fit to the ME spectrum (2–6 keV) which they determine to be $\alpha_{ME} = -0.96 \pm 0.06$.

An important discovery of CWG, the one which governs the current study, is that a strong correlation exists between the ratios Lyα/C IV and Lyα/Mg II and the continuum flux at 1338 Å. Their linear regressions of the line ratios are

$$\text{Ly}\alpha/\text{C IV} = (1.96 \pm 0.07) + (0.080 \pm 0.007)F(1338\ \text{Å}), \quad (2)$$

$$\text{Ly}\alpha/\text{Mg II} = (3.89 \pm 0.14) + (0.27 \pm 0.02)F(1338\ \text{Å}), \quad (3)$$

where F(1338 Å) is the continuum flux at 1338 Å (in units of 10^{-14} ergs cm^{-2} s^{-1} Å^{-1} in CWG; all other fluxes below will be in units of ergs cm^{-2} s^{-1} Hz^{-1}). For the customary single cloud calculations, the factor of increase in U is equal to the flux increase factor Λf(1338 Å) if only the luminosity of the ionizing continuum, but not its shape, varies. The problem is, as CWG point out, that photoionization calculations predict an opposite relation between Lyα/C IV and f(1338 Å) to the one observed. To illustrate, we show in Table 1 the typical behavior of Lyα/C IV when U is increased. Here the ionizing distribution is AD30X and is described below ($E_{eV} = 30$ eV, but note that $\rho_{912} = 0.10$; see § IV). To establish a point of reference, let us define the reprocessing efficiency η_{line} of the ionizing radiation Q_t (eq. [1]) into a given line of flux f_{line} (ergs cm^{-2} s^{-1}) as

$$\eta_{line} = (Un_H)^{-1} f_{line},$$

which, for optically thin recombination lines, would be nearly constant over a wide range in U and n_H. We see in Table 1 that

TABLE 1

EMISSION-LINE RATIOS FOR THE IONIZING CONTINUUM AD30X[a]

	Single Cloud, $n_H = 10^{10.5}$ cm^{-3}						Distribution in U and n_H	
U	$\eta_{Ly\alpha}$	$\eta_{C\,IV}$	$\eta_{Mg\,II}$	Lyα/C IV	Lyα/Mg II	$\bar{U}_{1/2}$[b]	Lyα/C IV	Lyα/Mg II
5.0×10^{-4}.....	0.78	0.00056	0.11	1380	6.8	5.0×10^{-4}	19.0	23.2
1.0×10^{-3}.....	0.74	0.0041	0.10	177	7.1	...	...	...
1.7×10^{-3}.....	0.73	0.015	0.10	49.4	7.4	1.7×10^{-3}	7.9	20.0
5.0×10^{-3}.....	0.67	0.081	0.083	8.3	8.1	...	...	...
1.0×10^{-2}.....	0.62	0.15	0.085	4.3	7.2	...	...	...
1.7×10^{-2}.....	0.57	0.20	0.083	2.9	6.9	1.7×10^{-2}	2.6	20.8
5.0×10^{-2}.....	0.42	0.26	0.054	1.6	7.9	...	...	...
1.0×10^{-1}.....	0.35	0.26	0.035	1.3	9.8	...	...	...
1.7×10^{-1}.....	0.30	0.25	0.026	1.2	11.9	...	...	...
5.0×10^{-1}.....	0.24	0.20	0.013	1.2	18.9	...	...	...

[a] Continuum with cutoff $E_{eV} = 30$ eV and $\rho_{912} = 0.10$.

[b] $\bar{U}_{1/2}$ is the ionization parameter at the radius of half-power in He II luminosity.

$\eta_{\rm C\,IV}$ increases very steeply with U, while $\eta_{\rm Ly\alpha}$ is a slowly decreasing function. At BLR densities the collisionally excited C IV resonance line is a major coolant which acts as a "thermostat" for the plasma; the onset of cooling by C IV depends critically, however, on the flux density of photons above 48 eV necessary to produce the species C^{+3}. The idea behind changing the energy distribution so that Lyα/C IV increases instead is to prevent any significant increase in the flux of photons of energy above 48 eV while f(1338 Å) is increasing. The slow decrease in $\eta_{\rm Ly\alpha}$ with U in Table 1 results from Lyα saturation, i.e., large optical depth in the line. From Table 1 it is obvious that when the luminosity of the continuum alone changes, Lyα/C IV must decrease as the UV increases. The variation of Lyα/Mg II with U, on the other hand, is much less pronounced and can present a secondary maximum around $U \simeq 10^{-3}$ whose importance depends on the gas density adopted. With the value of $n_{\rm H} = 10^{10.5}$ cm^{-3} adopted for all the calculations below, within a certain range Lyα/Mg II can increase with U; this ratio is thus not as relevant as Lyα/C IV in our effort to determine how the continuum might be evolving. Similar calculations at $10^{9.5}$ convinced us that high densities were useful but not essential in getting Lyα/C IV to increase with f(1338 Å), which was, in our estimation, the main difficulty.

IV. APPROACH CHOSEN IN VARYING THE IONIZING CONTINUUM

Instead of making a general comparative study of different ionizing distributions like Krolik and Kallman (1988) and Kallman and Elitzur (1988), we have taken the line of following the emission-line spectrum of a given ionized cloud, as the energy distribution to which it is exposed evolves in shape and luminosity in a prescribed manner. The basic aim is to determine how the ionizing continuum must change in order to invert the natural tendency of Lyα/C IV to increase steadily with f(1338 Å) or U. To alter the energy distribution, we resort to a two-component energy distribution with each component exhibiting a distinct luminosity behavior with time. One component, the secondary ionizing component, extends, and dominates the X-rays, and the other, the primary component, is an extension of the UV bump and dominates the 4–40 eV region. The complete ionizing continuum is simply the algebraic sum of these two components.

Our X-ray component will consist of a power law of index α_X with no low-energy cutoff, as we considered that an ad hoc low-energy turnover would not be warranted in the current exploratory study. The luminosity level of this secondary (X-ray) component in relation to the (primary) UV bump is completely specified by our parameter ρ_{912} which is the fractional flux contribution to the sum of the two components (at 1 Ry). As we considered it important to be able to vary the hardness of the primary component or UV bump, we chose a distribution for the UV which presents a *smooth* cutoff ($E_{\rm eV}$) in the EUV. To this end, the following function with an exponential cutoff was adopted:

$$f_\nu \propto \nu^{1/3} \exp\,(-h\nu/E_{\rm eV})\,, \qquad (4)$$

which also describes reasonably well the characteristic accretion disk energy distribution. In § V*b*, we will introduce more physical distributions using slim disk accretion models in which both the luminosity and the energy distribution evolve according to the variation in the accretion rate.

The luminosity light curve of the composite distributions will be expressed in terms of the temporal behavior of the flux at 1 Ry which impinges on the cloud: f(912 Å) (see eq. [1]). The choice of 912 Å rather than 1338 Å as the reference wavelength is only a matter of convenience and has no bearing on the conclusions. Given that it is the primary component which we vary by a factor of 33 and that we have not imposed a low-energy cutoff to the power law, the evolutionary sequence of the composite distributions result in a smaller Λf(1338 Å) of $\approx$27; we have verified, however, that not having (the composite) Λf(1338 Å) of exactly 33 does not weaken the conclusions reached below. We note, finally, that we adopted the convention of ordering the distributions from low to high state so as to simplify the discussion of ratios which increase with increasing flux, although the observations actually present the chronologically inverse evolution from high to low state.

V. MODEL RESULTS AND DISCUSSION

a) Varying the Luminosity of the Primary Component

First, we will consider evolutionary sequences where each sequence consists of five energy distributions in which the UV bump component increases in flux [f(912 Å)] by successive factors of 1.0, 2.4, 5.8, 13.8, and 33.0, while the secondary (X-ray) component is maintained at constant flux luminosity. The secondary component is set to contribute 15% to the low state (i.e., first) distribution of a sequence and proportionally less in the four subsequent distributions because the X-ray flux is constant. This low state value of ρ_{912} is an estimate of the extrapolated ME power-law of the 1984 October 25 *EXOSAT* data of Morini *et al.* (1986). The energy distribution corresponding to the low state of each sequence is plotted in Figure 1. In all the photoionization calculations presented below, the ionization parameter at low state is $U_{\rm low} = 0.02$. Although this implies somewhat large values of U for the high state, Krolik and Kallman (1988) have corroborated that distributions with a soft bump operate best at a high ionization parameter with respect to the goodness of the fit to observed line ratios. Furthermore, physical arguments concerning the maximum value that U can take without destroying the cloud cannot be strictly applied to objects where the high state is possibly only a transient phase.

In Table 2, models i–v of the sequence AD30X show how line ratios behave when the distribution consists of a "hot" primary component with $E_{\rm eV} = 30$ eV added to an X-ray power law of index $\alpha_X = -1.0 (\approx \alpha_{\rm ME})$. There is no apparent trend in the behavior of Lyα/C IV as a function of f(912 Å). On the other hand, the second sequence AD10X, comprising models 1–5, corresponds to calculations where the primary component is "cooler" with $E_{\rm eV} = 10$ eV. It turns out that the AD10X sequence is quite successful in producing a monotonic increase of Lyα/C IV. A linear fit of the calculated Lyα/C IV as a function of f(912 Å) gives a slope, if converted to the units used by CWG (eq. [2]), of $m' = 0.11$, as indicated in Table 3. Although the increase is monotonic and the slope comparable to the data of CWG, it should be added that Lyα/C IV does not strictly follow a straight line. However, given the radical simplification in the geometry of the BLR implicit in single cloud calculations, our results are very significant and highlight the important role played by the luminosity and temporal behavior of the very soft X-rays (50–300 eV).

To show that the harder X-rays are much less germane to the Lyα/C IV problem, we have calculated the sequence AD10XM, models A–E, with an $\alpha = -0.7$ power law below 300 eV but with a discontinuous break at this point to a

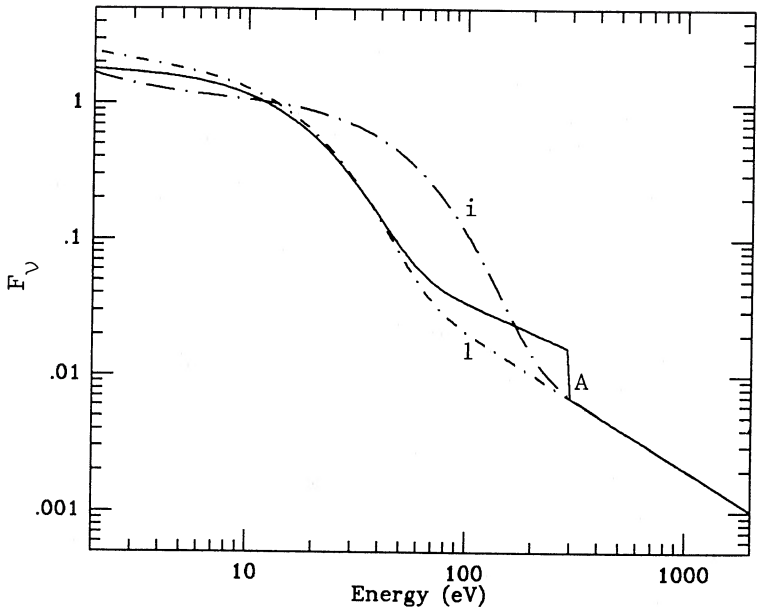

FIG. 1.—Ionizing energy distributions F_ν (in arbitrary units) of the low state continua in Table 2: AD30X(i), AD10X(1), AD10XM(A). The distributions have been renormalized so that they overlap at X-ray energies.

power-law with $\alpha_X = -1.0$ for energies above 300 eV. This sequence simulates a constant flux soft X-ray excess (see Fig. 1). The increase of Lyα/C IV with f(912 Å) is preserved because the abundance of the specie C^{+3} is essentially governed by photons of energy very much less than 300 eV.

We see that it is possible to counteract the effect of increasing the ionization parameter and still ensure that Lyα/C IV increases with f(912 Å) by making the overall energy distribution become progressively softer as it becomes more luminous; "softer" in the sense that there is proportionally less energy from the harder secondary component compared to the UV bump, as was initially proposed by CWG. What happens is that the flux density of photons of energy greater than 48 eV (but $\ll$ 300 eV) which produce C^{+3} and thereby determine the strength of C IV, increases relatively little if the X-ray component does not follow the luminosity increase of the primary UV component. This is because, with a sufficiently cool bump, most of the photons between 50 and 120 eV stem from the secondary rather than the primary component (see Fig. 1).

The success of the second sequence suggests that a cooler primary component with an even smaller cutoff would also work, since it would further increase the secondary component's contribution to the 50–120 eV region. However, this would result in a continuum with a much too steep UV spectral index (between 1826 and 1338 Å) which for AD10X is already a bit steeper than the observed α_{UV}. In order to maintain an acceptable α_{UV}, a different expression for the primary component in equation (4) would have to be employed, one characterized by a steeper cutoff or an α_{UV} relatively independent of E_{eV}, or both.

In all three sequences, we find that Lyα/Mg II increases with f(912 Å) rather more steeply than Lyα/C IV does. If, as is customary in BLR models, we consider the photoionized clouds to be matter bounded, the slope increases with decreasing N_H

TABLE 2

EMISSION-LINE RATIOS FOR IONIZING CONTINUA IN WHICH ONLY THE PRIMARY COMPONENT VARIES

PARAMETER	AD30X $E_{eV} = 30$ $\alpha_X = -1.0$					AD10X $E_{eV} = 10$ $\alpha_X = -1.0$					AD10XM $E_{eV} = 10$ $\alpha_X = -0.7, -1.0$				
Identification	(i)	(ii)	(iii)	(iv)	(v)	(1)	(2)	(3)	(4)	(5)	(A)	(B)	(C)	(D)	(E)
Λf(1338 Å)	1.0	2.1	4.8	11.3	26.8	1.0	2.2	5.0	11.8	27.9	1.0	2.2	5.1	11.9	28.3
Λf_x	1.0	1.0	1.0	1.0	1.0	1.0	1.0	1.0	1.0	1.0	1.0	1.0	1.0	1.0	1.0
α_{UV}	−0.28	−0.09	0.01	0.05	0.07	−0.88	−0.81	−0.77	−0.76	−0.76	−0.80	−0.77	−0.76	−0.75	−0.75
$\rho_{912}/10^{-2}$	15.0	6.8	3.0	1.3	0.53	15.0	6.8	3.0	1.3	0.53	15.0	6.8	3.0	1.3	0.53
f(912 Å)/10^{-8}	0.83	1.8	4.2	9.9	23.5	1.6	3.5	8.0	19.1	45.3	1.5	3.2	7.4	17.4	41.2
$U/10^{-2}$	2.0	4.5	10.3	24.4	58.0	2.0	4.3	9.2	21.5	50.6	2.0	3.9	8.5	19.7	46.2
Lyα/C IV	2.3	1.7	1.6	1.8	2.2	4.7	4.7	5.1	5.8	7.2	3.2	3.5	4.1	5.0	6.6
Lyα/Mg II	9.9	14.1	25.4	57.4	84.6	5.7	7.0	9.2	15.8	10.4	5.9	7.0	9.6	16.5	11.6
Lyα/Mg II[a]	9.9	14.7	26.7	60.9	127	6.4	9.1	16.0	37.7	55.1	6.5	8.7	15.4	38.1	54.7
C III]/C IV	0.38	0.28	0.25	0.28	0.38	0.79	0.82	0.88	1.04	1.5	0.60	0.65	0.72	0.90	1.3

[a] Lyα/Mg II for the density-bounded case with $N_H = 10^{24.5}$ cm^{-2}.

TABLE 3

COEFFICIENTS OF THE LINEAR FIT[a] TO THE CALCULATED LINE RATIOS

Distribution	U_{low}	log N_H	Lyα/C IV			Lyα/Mg II		
			a	m	m'	a	m	m'
AD10X	0.020	24.5	4.6	5.83×10^6	0.11	7.4	1.12×10^8	2.1
AD10X	0.020	25.0	4.6	5.83×10^6	0.11	7.9	6.85×10^7	1.2
AD10X	0.020	26.0	4.6	5.83×10^6	0.11	...	...	...
AD10XM	0.020	24.5	3.3	8.29×10^6	0.14	7.2	1.24×10^8	2.1

[a] $r = a + mf(912\text{ Å}), m' \simeq 1.14mf(912\text{ Å})^{\text{low state}}$ to conform to definition of $F(1338\text{ Å})$ in eqs. (2)–(3).

as shown in Table 3 but for the sequence AD10X, it ensures, at least, a monotonic increase with $f(912$ Å).

As regard to the intercept of the linear fit in Table 3, the plausible sequence AD10X results in values of Lyα/C IV and Lyα/Mg II which are both too large by a factor of roughly 2 compared to equations (2)–(3). Increasing n_H does reduce Lyα/C IV and C III/C IV but rather than increasing U_{low} or n_H in an attempt to fine tune the line ratios, it would make better sense to explore a more realistic geometrical cloud distribution taking into account stratification of the cloud properties, which would alter not only the line ratios but possibly the slope as well.

b) *Varying the Secondary Component*

Although the constant flux secondary component gives good results, it is at odds with the X-ray observations which have reported long-term variability of the 2–6 keV count rate. In this section we relax the constancy of the X-ray component and show what happens when the X-ray flux is allowed to increase as well. This ends up overturning the qualitative agreement with the observed correlations previously achieved. Despite the occasional, initial Lyα/C IV increase with some distributions as $f(912$ Å) increases, the last model [high state with $\Lambda f(1338\text{ Å}) > 24$] invariably yields a smaller Lyα/C IV than the low state. To illustrate this, therefore, only the two calculations corresponding to the *low* and *high* state respectively will suffice.

The next calculations assume a factor of 4 increase (Λf_X) in the 2–6 keV ME flux to accompany the primary component increase of a factor of 33. Note that it corresponds to the minimum amount of variation inferred from X-ray observations if we limit ourselves to epochs where *IUE* was operational. The results presented in Table 4 clearly indicate Lyα/C IV to be smaller at high state for both sequences AD30Xv and AD10Xv which correspond to $E_{eV} = 30$ and 10 eV, respectively. Calculation 2′ shows that this result remains unchanged even with a much smaller $\Lambda f(1338$ Å) of 13.3. The decrease in Lyα/C IV is a simple consequence of the secondary component's directly governing the strength of C IV; when the latter increases we can expect Lyα/C IV to decrease at some point. Another problem is to establish the appropriate value of Λf_X, since the *EXOSAT* data indicates the very soft X-rays ($\ll 1$ keV) to have varied by 60% more than the 2–6 keV ME flux between 1983 and 1984. The problem is further exacerbated by the fact that $\Lambda f_X \geq 6$ would make it even more difficult to reproduce a monotonic increase in Lyα/C IV. Since very soft X-ray observations are not available for the period that Fairall 9 was at high state, we cannot rule out the possibility that the LE soft X-rays were actually weaker than that in other epochs. It would, however, be surprising for the trend observed during 1983–1984 to be reversed when Fairall 9 was closer to its peak.

We conclude that a monotonic increase in the secondary component, even by a factor as small as 4, cannot be suc-

TABLE 4

EMISSION-LINE RATIOS FOR IONIZING CONTINUA WHERE THE X-RAY FLUX VARIES AND FOR THE SLIM DISK MODEL

Name	AD30Xv		AD10Xv			AD30>10Xv				SliX[a]			
E_{eV}	30		10			30, 10							
α_X	−1.0		−1.0			−1.0				−1.0			
Id.	(i)	(ii)	(1)	(2)	(2′)	(a)	(b)	(b′)	(b″)	(A)	(B)	(C)	(D)
$\Lambda f(1338$Å$)$	1.0	24.9	1.0	25.9	13.3	1.0	27.4	27.0	26.6	1.0	1.5	2.6	9.0
Λf_X	1.0	4.0	1.0	4.0	4.0	1.0	8.0	6.0	4.0	1.0	1.0	1.0	1.0
α_{UV}	-0.28	0.03	-0.88	-0.77	-.79	-0.28	-0.80	-0.78	-0.77	-0.94	-0.71	-0.42	-0.38
$\bar{\varepsilon}$ (eV)	39.9	35.0	35.8	24.1	26.3	39.9	27.1	25.9	24.6	37.2	30.8	26.2	24.6
$\rho_{912}/10^{-2}$	15.0	2.3	15.0	2.3	4.5	15.0	5.3	4.1	2.7	15.0	9.4	5.1	1.6
$\sigma_Q/10^{-2}$	12.5	1.8	24.0	4.0	7.8	12.5	9.2	7.0	4.8	29.3	17.9	9.3	3.0
$f(912$Å$)/10^{-8}$	0.83	21.7	1.6	41.9	21.4	0.83	18.7	18.4	18.2	2.0	3.1	5.7	17.9
$U/10^{-2}$	2.0	53.5	2.0	47.5	24.7	2.0	21.7	21.2	20.7	2.0	3.3	6.3	19.8
Lyα/CIV	2.3	2.1	4.8	4.5	3.3	2.3	3.0	3.5	4.3	5.1	5.5	6.1	3.9
Lyα/MgII	10.2	43.1	5.7	9.7	9.4	10.2	9.1	9.0	9.7	5.2	6.1	8.5	14.8
Lyα/MgII[b]	10.2	76.1	6.5	36.4	20.5	10.2	18.2	20.2	25.2	6.1	7.5	11.9	30.5
CIII]/CIV	0.38	0.37	0.78	0.95	0.67	0.38	0.62	0.69	0.81	0.78	0.90	1.0	0.68

[a] Slim disk accretion model of viscosity $\alpha = 0.001$ for accretion rates of 0.03, 0.05, 0.1, and 1.0 $M_\odot$ yr^{-1} into a black hole of mass $1.0 \times 10^8 M_\odot$.

[b] Lyα/Mg II for the density bounded-case with $N_H = 10^{24.5}$ cm^{-2}.

cessfully accommodated in our dual components approach. There is an inconsistency between these results and the observations: on the one hand, to reproduce the observed line correlations, it appears that near constancy of flux in the 50–150 eV region is required and on the other hand, the 2–10 keV flux was definitely observed to vary in Fairall 9 by a factor of 4–7 (since 1970; see Table 6 in Morini *et al.*). This inconsistency may, however, be more apparent than real. A possible solution is provided by Morini *et al.* in one of their interpretations of the soft X-ray variability. They indicate that variations in the absorbing column density along the line of sight could account for the observed variability. The fact that the variability is in the direction of a larger column absorption as $f(1338$ Å) decreases is consistent with the "warm absorber" model of Halpern (1984), since the decreasing luminosity would reduce the ionization of the intervening absorbing material, enabling it to become more opaque to soft X-rays. If this interpretation is correct, BLR clouds in Fairall 9 may well have been exposed to the constant X-ray flux which our models favor to account for the line correlations. Yaqoob, Warwick, and Pounds (1988) have recently outlined in more detail the warm absorber model, as well as that of partial source covering, in an effort to interpret the spectral X-ray variability in NGC 4151 which similarly presents an anticorrelation between the X-ray luminosity and the absorbing column density or the soft X-ray excess.

c) *Varying the Hardness of the Primary Component*

If we want Lyα/C IV to increase despite a moderate increase in the X-rays, another avenue that can be taken is to have the primary component become softer within the sequence, that is, to have E_{eV} decrease with luminosity. The sequence AD30 > 10Xv takes this course with E_{eV} going from 30 eV at low state to 10 eV at high state. In Table 4 we show three different cases in terms of the factor Λf_X by which the high state X-ray luminosity has increased: 8.0(*b*), 6.0(*b'*) and 4.0(*b''*), respectively. The results indicate that the X-rays can indeed increase and still produce a larger Lyα/C IV at high state if the primary component becomes softer. A first problem, however, is that the UV spectral index changes dramatically along the sequence, from $\alpha_{UV} = -0.28$ to ≈ -0.78, which is at odds with *IUE* results: an unavoidable consequence of any energy distribution with a smooth cutoff since tampering with E_{eV} will alter the UV spectral slope. A more fundamental problem is that most of the physical emission mechanisms generally held responsible for the UV bump predict a hotter distribution at higher luminosity. One such physical model purporting to explain the big bump is the accretion disk model in which an increase in luminosity can be accounted for by an increase in the accretion rate. Sequence SliX, presented in Table 4, illustrates the self-consistent evolution from low to high state of an energy distribution emitted from a slim accretion disk (Szuszkiewicz 1988; Abramowicz *et al.* 1988). The viscosity is 0.001 and the mass of the assumed black hole is $1.0 \times 10^8 M_\odot$. At these parameters, the stability criterion for the slim disk model would imply an increase in the primary component flux, $f(912$ Å) of $\simeq 10.6$ for an increase in the accretion rate from 0.03 to 1.0 $M_\odot$ yr^{-1}. [Larger accretion rates at these particular parameters would only result in a harder distribution without further increase in $f(1338$ Å)]. It is apparent from Figure 2, that the secondary component becomes harder with $f(1338$ Å) but the mean ionization photon energy $\bar{\epsilon}$ (see Table 4) of the composite distribution nevertheless decreases with $f(1338$ Å). Table 4 also gives σ_Q, the fraction of ionizing photons (below 5 keV) which the secondary component contributes to the composite ionizing spectrum. Even without allowing the secondary component to vary and with a relatively small $\Lambda f(1338$ Å) of 9.0, the increase in Lyα/C IV is no longer monotonic, as shown by models A–D of the SliX sequence. This is obviously attributable to the progressive hardening of the primary component. We also note that the spectral index α_{UV} is not constant along the sequence although this discrepancy could conceivably disappear if a power law with a low-energy cutoff was used and the viscosity in the disk models was allowed to vary somewhat as the accretion rate increases.

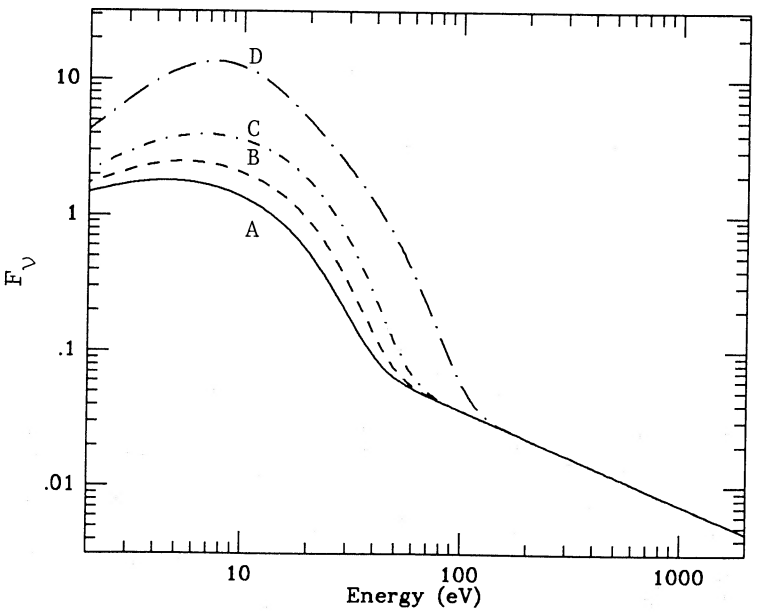

FIG. 2.—Ionizing energy distribution F_ν (arbitrary units) of the slim accretion disk sequence of Table 4: SliX (A), (B), (C), (D)

d) Influence of Geometrical Parameters

It is worth considering whether an explicit geometrical distribution of clouds can affect the above constraints placed on the secondary component's behavior. With a sufficiently thick BLR, as in the models of Binette *et al.* (1989), different lines tend to be emitted preferentially at the radius where the reprocessing efficiency is highest. As a result, when the central UV source drastically increases in luminosity, the thickness or weighted contribution of the various emission zones corresponding to the different lines does not increase linearly with $f(1338\ \text{Å})$. The following geometrical model of a thick BLR, computed using the code OBFRAM developed by Robinson (1989), confirms the need to pursue our exploration of these effects. This test model consists of 24,500 clouds distributed at random within a sphere of inner radius of 50 light-days and outer radius of 5000 light-days; the space density of clouds (as well as n_H of each cloud) decreases as $1/r$ from the UV source which in this instance is nonvariable; the line emissivity of each cloud was obtained from MAPPINGS as in the single cloud case above. Note that this rather large BLR size is not necessarily in contradiction with the small time lags, in some AGN, in the emission-line response to continuum variability, as recently shown by Robinson and Pérez (1989). The near constancy of Lyα/Mg II in the geometrical model of Table 1 might be seen as a further indication that the observed line ratio evolution in Fairall 9 cannot be satisfactorily explained without changing the energy distribution; it also suggests that the too large slope of Lyα/Mg II in Table 3 might not be a problem at all when BLR stratification is considered. Another interesting feature of the thick BLR calculations in Table 1 is that an increase in U by a factor of 10 results in a significantly smaller increase in Lyα/C IV than in single cloud calculations. (A similar initial Lyα/C IV has to be chosen for this comparison to be meaningful). The cloud system as a whole is characterized by a reduced dependency on U. This gives rise to the possibility that, replacing the single cloud approach by a more realistic geometry, might suffice to diminish to some degree the constraints on the evolution of the ionizing continuum: some hardening of the primary component or some increase in the soft X-rays might take place without hindering the reproduction of the observed line ratio correlations—a lead not to be neglected in future calculations.

VI. CONCLUSION

Using standard parameters to describe a broad-line region cloud, we have indicated a possible evolutionary sequence of the ionizing energy distribution which is able to counteract the otherwise dominant dependency of Lyα/C IV on the ionization parameter. This sequence is characterized by a 10 eV bump only marginally steeper than observed by *IUE* but it requires the very soft X-ray (50–300 eV) power law to remain constant in luminosity. The latter requirement may not necessarily be at odds with the *EXOSAT* observations if variations in the absorbing column density are considered. In our view, it would be appropriate to use similar evolutionary sequences in future calculations but within the framework of a three-dimensional distribution of clouds. This would constitute a further check of the validity of the constraints imposed on the soft X-ray variations and of the usefulness of UV distributions, such as accretion disks, which becomes slightly harder with luminosity.

Thanks to the code OBFRAM of Andrew Robinson (IoA), we were able to calculate line emission spectra produced by three-dimensional geometrical distribution of clouds. We are indebted to the Instituto de Astrofísica de Canarias, our host during this collaboration, which provided generous allocation of computer CPU and disk space. We aknowledge financial support from the NATO collaborative research grant No. 0219/88.

REFERENCES

Abramowicz, M. A., Czerny, B., Lasota, J. P., and Szuszkiewicz, E. 1988, *Ap. J.*, **332**, 646.
Abramowicz, M. A., and Szuszkiewicz, E. 1989, in *Proc. Big Bang, Active Galactic Nuclei, and Supernovae*, ed. S. Hayakawa and K. Sato (Tokyo: Universal Academy Press), in press.
Binette, L., Robinson, A. 1987, *Astr. Ap.*, **177**, 11.
Binette, L., Robinson, A., and Courvoisier, T.-L. 1988, *Astr. Ap.*, **194**, 65.
Binette, L., Robinson, A., Zheng, W., Rodríguez Espinosa, J. M., and Pérez, E. 1989, in preparation.
Camenzind, M., and Courvoisier, T. J.-L. 1983, *Ap. J. (Letters)*, **266**, L83.
Clavel, J., Wamsteker, W., and Glass, I. 1989, *Ap. J.*, **337**, 236 (CWG).
Elvis, M., Green, R. F., Betchtold, J., Schmidt, M., Neugebauer, G., Soifer, B. T., Matthews, K., and Fabbiano, G. 1986, *Ap. J.*, **310**, 291.
Ferland, G. J., and Rees, M. J. 1988, *Ap. J.*, **332**, 141.
Halpern, J. P. 1984, *Ap. J.*, **281**, 90.
Kallman, T., and Elitzur, M. 1988, *Ap. J.*, **328**, 523.
Krolik, J. H., and Kallman, T. R. 1988, *Ap. J.*, **324**, 714.
Kwan, J., and Krolik, J. H. 1981, *Ap. J.*, **250**, 478.
Morini, M. 1986, *Ap. J.*, **307**, 486.
Mushotzky, R., and Ferland, G. J. 1984, *Ap. J.*, **278**, 558.
Robinson, A. 1989, in preparation.
Robinson, A., and Pérez, E. 1989, *M.N.R.A.S.*, submitted.
Szuszkiewicz, E. 1988, Ph.D. thesis, SISSA, Trieste.
Wamsteker, W., *et al.* 1984, in *Proc. 4th European IUE Conf.* (Rome), ESA SP-218, p. 97.
Yakoob, T., Warwick, R. S., and Pounds, K. A. 1988, preprint.
Zheng, W. 1989, *Ap. J.*, **337**, 617.

Luc Binette: CITA, 60 St George Street, University of Toronto, Toronto, Ontario M5S 1A1, Canada

Almudena Prieto: ESO, Karl-Schwarzschild Strasse 2, D-8046 Garching bei München, West Germany

Ewa Szuszkiewicz: MPA, Karl-Scwarzschild-Strasse 1, D8046 Garching bei München, West Germany

Wei Zheng: Department of Astronomy, University of Alabama, 206 Gallalee Hall, Box 1921, Tuscaloosa, AL 35487